The unresolved fine structure resolved: IRIS observations of the solar transition region

Authors: V. Hansteen, B. De Pontieu, M. Carlsson, J. Lemen, A. Title, P. Boerner, N. Hurlburt, T. D. Tarbell, J. P. Wuelser, T. M. D. Pereira, E. E. De Luca, L. Golub, S. McKillop, K. Reeves, S. Saar, P. Testa, H. Tian, C. Kankelborg, S. Jaeggli, L. Kleint, and J. Martínez-Sykora

The unresolved fine structure resolved: IRIS observations of the solar transition region

V. Hansteen,[1]* B. De Pontieu,[1,2] M. Carlsson,[1] J. Lemen,[2] A. Title,[2] P. Boerner,[2]
N. Hurlburt,[2] T. D. Tarbell,[2] J. P. Wuelser,[2] T. M. D. Pereira,[1] E. E. De Luca,[3] L. Golub,[3]
S. McKillop,[3] K. Reeves,[3] S. Saar,[3] P. Testa,[3] H. Tian,[3] C. Kankelborg,[4] S. Jaeggli,[4]
L. Kleint,[5,2] J. Martínez-Sykora[5,2]

The heating of the outer solar atmospheric layers, i.e., the transition region and corona, to high temperatures is a long-standing problem in solar (and stellar) physics. Solutions have been hampered by an incomplete understanding of the magnetically controlled structure of these regions. The high spatial and temporal resolution observations with the Interface Region Imaging Spectrograph (IRIS) at the solar limb reveal a plethora of short, low-lying loops or loop segments at transition-region temperatures that vary rapidly, on the time scales of minutes. We argue that the existence of these loops solves a long-standing observational mystery. At the same time, based on comparison with numerical models, this detection sheds light on a critical piece of the coronal heating puzzle.

The outer solar atmosphere between the 10^4 K chromosphere and the 10^6 K corona, the so-called transition region, has long puzzled solar physicists (1). It has been difficult to reconcile measured intensities and motions, either directly observed or inferred from spectra, with models of the energy and mass exchange between the cooler chromosphere and hot corona. For one, the observed intensities of lower transition-region lines are much greater than can be accounted for by thermal conductive flux flowing back from the corona. Furthermore, lower transition-region lines show, on average, Doppler redshifts on the order of 10 km/s (1), one-third the speed of sound. Based on indirect spectroscopic evidence from High-Resolution Telescope Spectrograph (HRTS) and Skylab spectra, it was already postulated in 1983 that the dominant emission from lines formed in the transition region occurs in structures magnetically isolated from the corona called the "unresolved fine structure" (UFS) (2–5). However, the following decades have not brought consensus that the UFS has been directly observed, nor indeed that it contributes to an important extent to transition-region emission (6–10). As a result, our understanding of coronal heating has not advanced substantially.

We exploit the high spatial and temporal resolution of the recently launched Interface Region Imaging Spectrograph (IRIS) satellite to reveal structures remarkably similar to those postulated to comprise the UFS. Images of the lower transition region at the solar limb with the IRIS slit-jaw camera (11) in the Si IV 1400 Å filter or in the C II 1330 Å filter invariably show bright low-lying loops or loop segments in quiet Sun regions (Fig. 1 and movies S1 and S2). In addition to these bright structures, a much fainter component forms a background that extends up to 10 arcsec above the limb. The background includes a large number of linear structures, with properties similar to the well-known spicules observed from the ground in the Hα 656.3-nm line. Here, we concentrate on the brighter loop-shaped objects that appear to be magnetically isolated from the corona and are at transition-region temperatures.

Viewing the same limb with the Solar Dynamics Observatory Atmospheric Imaging Assembly (SDO/AIA) instrument (12) in the 304 Å channel (which is dominated by He II, at 100,000 K) and the coronal 171 Å (Fe IX/X at ~10^6) and 193 Å (Fe XII at ~1.5 10^6 K) channels (13), we do not clearly observe UFS-related structures (Fig. 1 and movie S3). This is for two reasons: (i) the AIA spatial resolution is insufficient to resolve the structures discussed here, and (ii) bound-free absorption by neutral hydrogen and singly ionized helium renders the AIA opaque to extreme ultraviolet emission, thereby shielding the lower transition region and making the UFS nearly invisible.

One of the most striking features of UFS loops is temporal variability. Isolated UFS loops light up, either partially or wholly, and show large

[1]Institute of Theoretical Astrophysics, University of Oslo, Post Office Box 1029, Blindern, NO-0315, Oslo, Norway. [2]Lockheed Martin Solar and Astrophysics Laboratory, 3251 Hanover Street, Org. A021S, Building 252, Palo Alto, CA 94304, USA. [3]Harvard-Smithsonian Center for Astrophysics, 60 Garden Street, Cambridge, MA 02138, USA. [4]Department of Physics, Montana State University, Bozeman, Post Office Box 173840, Bozeman, MT 59717, USA. [5]Bay Area Environmental Research Institute, 596 1st Street West, Sonoma, CA 95476, USA.
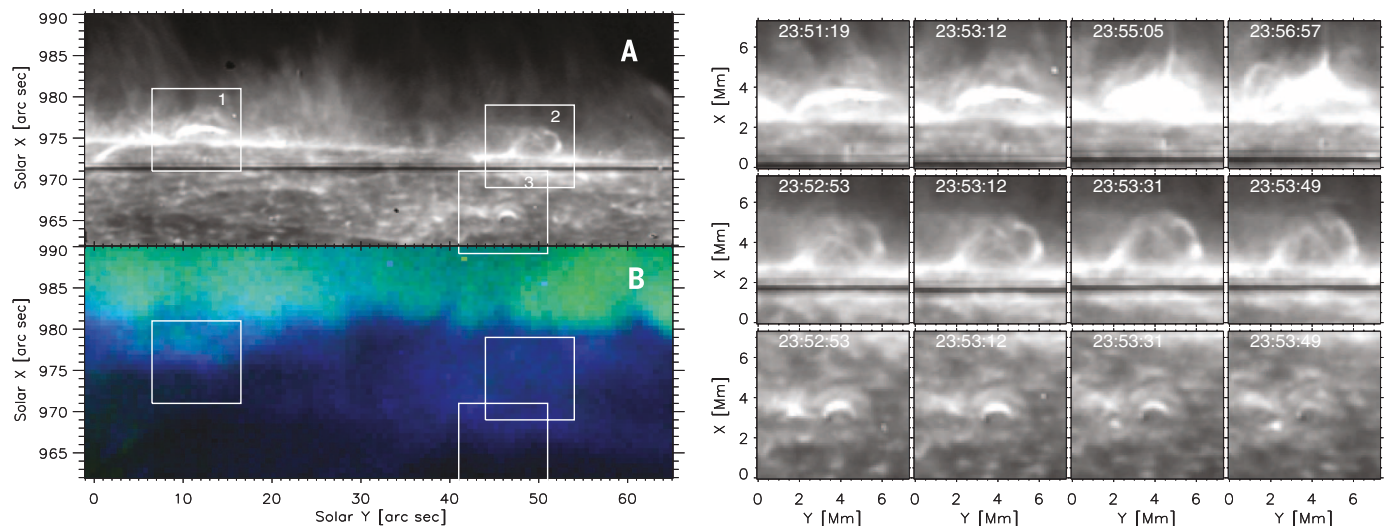*Corresponding author. E-mail: viggoh@astro.uio.no

Fig. 1. IRIS Si IV 1400 Å slit jaw images reveal highly dynamic, low-lying loops at transition-region temperatures. (**A**) UFS loops on the western solar limb. The slit is evident as a dark line near solar-x = 971 arcsec. (**B**) The same field of view is shown, but with SDO/AIA images: the coronal 171 Å (blue) and 193 Å (green) filters (movie S3 shows the same field of view, but with the AIA He II 304 Å filter). The rapid evolution of the UFS in three ROIs is demonstrated in the small panels on the right side of the figure. The time of each exposure (hour:minute:second) is indicated at the top of the panels.

changes on scales down to the shortest cadence data inspected so far (every 4 s), examples of which are shown in region of interest (ROI) 2 and ROI 3 of Fig. 1. On the other hand, a system of loops, in which individual loops vary from exposure to exposure, can remain recognizable as a system over periods extending to several tens of minutes. The temporal evolution of the three regions of interest are shown in Fig. 1 (more loops are displayed in fig. S1). ROI 1 was observed with

Fig. 2. UFS loops are short, bright, and low-lying. Properties of 85 UFS loops taken from a limb observation data set: (**A**) apparent length of the visible loop segments, (**B**) projected full length along loop, (**C**) maximum height, and (**D**) median intensity of the visible loop segments. The intensity measured for the dimmer "spicular" background is shown with a dashed line.

a cadence of 54 s and is an example of a fairly long-lived "nest" of loops that remains active during the entire 40-min span that the observations lasted. Movies S1, S2, and S3 show these nests to be composed of many loops with more or less cospatial footpoints that light up and darken episodically.

Fully formed loops are seldom seen. Rather, loops appear to be lit up in segments, with each segment only being visible for roughly a minute. There is also a tendency for the UFS loops to appear to rise with time, as can be seen in ROI 2 (Fig. 1).

We find that the UFS loops have a full length of 4 to 12 Mm (10^6 meters), a maximum height of 1 to 4.5 Mm with an average of 2.5 Mm, and a median intensity in data numbers per second of 40 to 50 DN/s (Figs. 2) (*14*). This intensity is larger than the measured intensity of the background "spicules"—longer nearly radial features—of 15 DN/s, which is also apparent from visual inspection of Fig. 1. Although the detailed filling factor of either component is not well known (given the superposition at the limb and their limited visibility on the disk), it is clear that both resolved components have an important role in the lower transition-region emission, with the relative contribution dependent on the local magnetic field topology.

By aligning the slit along the limb, IRIS also allows one to gather spectral data of the UFS (example in Fig. 3). The spectrum shows large excursions as a function of position along the loop, implying large plasma velocities, toward the red as well as toward the blue. We find extreme line profiles at the upper loop footpoint—the portion of the loop that meets the underlying atmosphere—during the entire 200-s lifetime of the UFS loop, with redward excursions of 70 to 80 km/s. This is two to three times the speed of sound in a 80,000 to 100,000 K plasma. We observed the spectral properties of several UFS loops and find that such high velocities occur often, although not always. This indicates that the UFS loops are locations of episodic and violent heating.

How can we put these observations into the context of coronal heating models and the structure of the upper solar atmosphere? Models that assume most transition-region emission stems from loops connected to the corona, and therefore whose temperature structure is maintained by thermal conduction, lead to predicted intensities much smaller than those observed. Alternative models propose the existence of low-lying cool loops (*15–17*), but these static models cannot be reconciled with the highly dynamic loops we observe here. Guidance comes from three-dimensional (3D) modeling: Low-lying, episodically heated loops that seldom or never reach coronal temperatures naturally arise in 3D models and predict (*18–20*) highly dynamic spectral lines originating in the lower transition region. Thus, several properties of UFS loops are remarkably similar to those found in recent realistic 3D models spanning the convection zone to the corona.

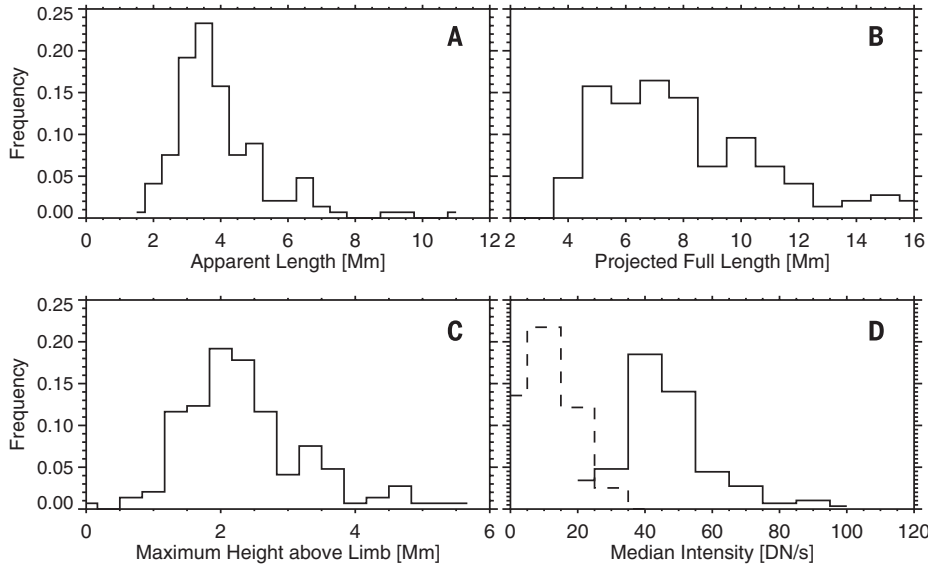The typical loop height of the brightest cool loops that spontaneously arise in 3D simulations
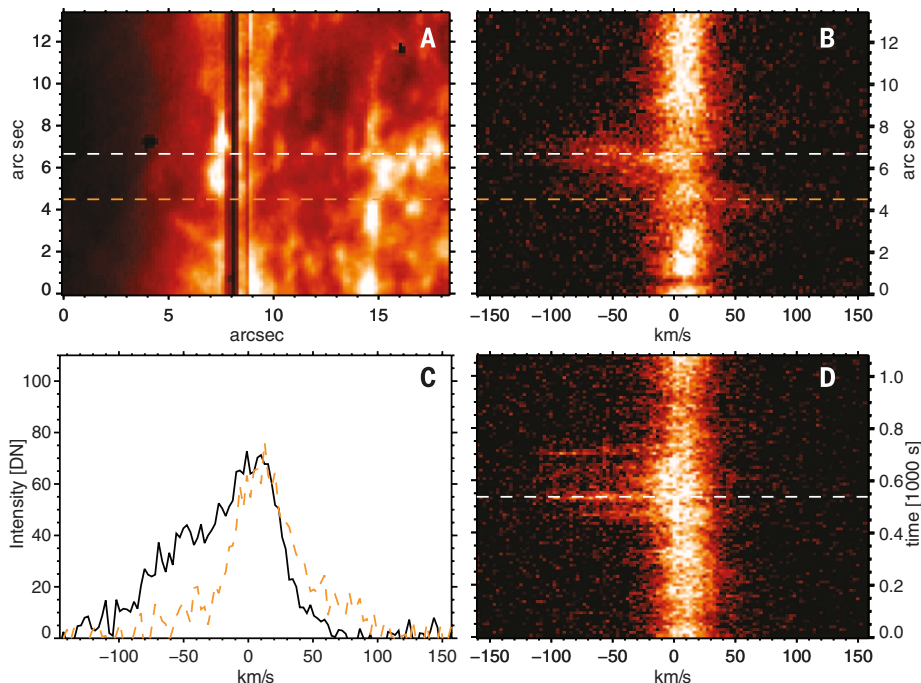

Fig. 3. UFS loops display large, rapidly evolving Doppler shifts and nonthermal velocities. (**A**) The slit position along the limb (SJI 1400 Å). (**B**) The corresponding spectral scans of the Si IV 1393 Å line are shown as a function of position along the slit and as a function of time at the location of the UFS loop footpoint (**D**) located at 6.6 arcsec. In (**B**) and (**D**), the dashed white and orange lines show the locations of the footpoints. (**C**) The corresponding line profiles at these footpoint locations (540 s) are shown in solid and gold dashed curves, respectively.
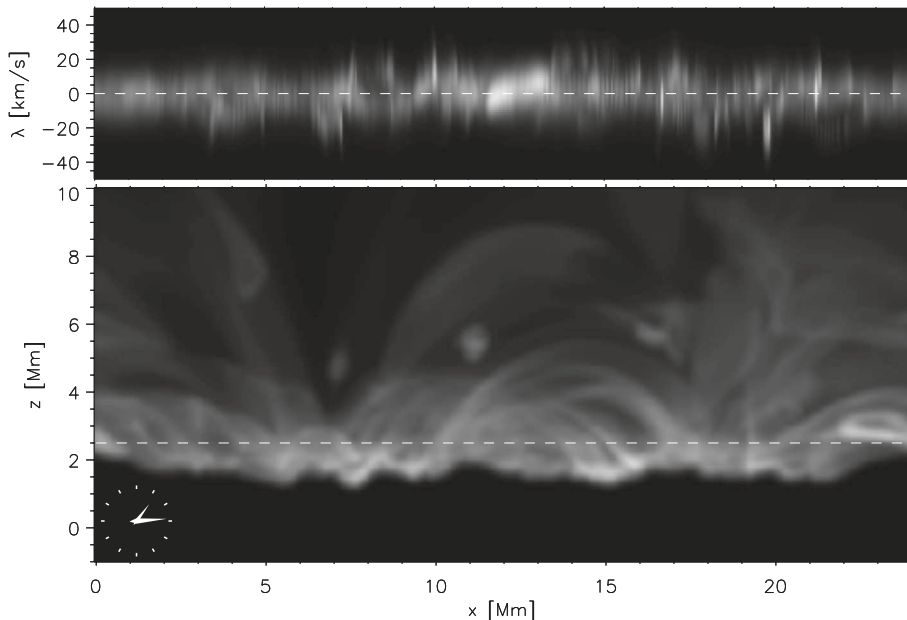
Fig. 4. Episodic structures with properties similar to UFS loops arise in advanced 3D numerical simulations. The synthetic line profile of the Si IV 1393 Å line (**top**) and the corresponding synthetic intensity images of the solar limb (**bottom**) are shown. The dashed white line in the lower panel shows the location sampled for the synthetic spectrum. The resolution of the intensity images has been degraded to the IRIS spatial resolution of 0.33 arcsec. Movie S4 shows the temporal evolution of this simulation.

(Fig. 4) is less than 4 Mm above the photosphere. The lifetime of individual "strands," or loops, that maintain plasma in the temperature range required for emission in the Si IV line is a few hundred seconds or less. Both of these properties are very similar to what is observed. However, Doppler velocities measured at the origin of the line profile show line-of-sight velocities on the order of 20 to 30 km/s, which is less than that reported for our observations.

Why do these loops form? Heating in the upper chromosphere and corona will proceed along and be guided by the loop magnetic field. This could occur either through the dissipation of waves or through the dissipation of stresses built up as a result of footpoint motions (*21*). Whereas long loops lose energy through thermal conduction, shorter loops are denser at their apices and will therefore lose energy efficiently through radiative losses, which scale as the density squared [e.g., (*18*, *19*, *20*)]. The cooling time of low-lying loops is short (a few minutes or less), and a reduction in the heating rate ensures rapid cooling. At heights of 5 Mm or less above the photosphere, these models therefore predict short low-lying loops that are episodically heated to ~500,000 K or less. The loops cool rapidly thereafter rather than being heated to coronal temperatures.

The discrepancy between observed and modeled velocities could be an indication that the models correctly predict the spatial distribution and episodic nature of the heating in the corona, but the detailed nature of the heating mechanism may not be exactly reproduced. The spatial distribution of loops is largely independent of the heating mechanism and is instead set by the structure of the field. We thus expect low-lying

loops to occur in any realistic 3D model. However, the temporal properties of the loop emission or Doppler velocities are a direct result of the heating process, and comparison of synthesized and observed data could validate a given model.

What sets the low height of the observed loops? It is likely that these dynamic small-scale loops in the low solar atmosphere are associated with ubiquitous weak magnetic field in the solar photosphere (*22*–*24*). These continuously emerging weak fields occur on granular scales, with opposite polarities separated by a few Mm. Our observations of the low loop heights and the sometimes persistent "nests" of loops are fully compatible with theoretical predictions. If such weak fields are present, they should form a multitude of dynamic low-lying loops (*16*), especially when they interact with the strong magnetic field in the quiet Sun network (*25*). The apparent rise of some of the observed loops is likely caused by the emergence of the loops into the atmosphere (*26*).

Based on their properties, and in comparison with 3D models, we conclude that the short low-lying loops observed with IRIS constitute a set of low-lying magnetic structures whose plasma is episodically heated. The thermal properties of these loops are determined by their high density, which causes efficient radiative cooling and thus prevents the occurrence of coronal temperatures. Higher-lying loops are presumably heated in much the same way, but with radiative losses that are much less efficient at lower densities, and temperatures must rise to > 1 MK to balance heating with losses due to thermal conduction. By revealing the existence and properties of these previously unresolved fine-structured loops, we have obtained direct

insight into the otherwise difficult to observe coronal heating mechanism. The episodic nature, height distribution, and high velocities of UFS loops provide strict constraints on recent 3D models of the coronal heating problem. Further observations and more advanced modeling of these loops are critical for determining the relation between the topology of the magnetic field in the photosphere and vigorous heating in the outer atmosphere.

REFERENCES AND NOTES

1. J. Mariska, *The Solar Transition Region*, Cambridge Astrophysics Series (Cambridge Univ. Press, New York, 1992).
2. U. Feldman, On the unresolved fine structures of the solar atmosphere in the 30,000-200,000 K temperature region. *Astrophys. J.* **275**, 367 (1983). doi: 10.1086/161539
3. U. Feldman, On the unresolved fine structures of the solar atmosphere. II. The temperature region 200,000 - 500,000 K. *Astrophys. J.* **320**, 426 (1987). doi: 10.1086/165556
4. U. Feldman, K. G. Widing, H. P. Warren, Morphology of the quiet solar upper atmosphere in the $4 \times 10^4 < T_e < 1.4 \times 10^6$ K temperature regime. *Astrophys. J.* **522**, 1133–1147 (1999). doi: 10.1086/307682
5. U. Feldman, I. E. Dammasch, K. Wilhelm, On the unresolved fine structures of the solar upper atmosphere. IV. The interface with the chromosphere. *Astrophys. J.* **558**, 423–427 (2001). doi: 10.1086/322471
6. J. Dowdy, Observational evidence for hotter transition region loops within the supergranular network. *Astrophys. J.* **411**, 406 (1993). doi: 10.1086/172842
7. Ø. Wikstøl, P. Judge, V. Hansteen, On inferring the properties of dynamic plasmas from their emitted spectra: The case of the solar transition region. *Astrophys. J.* **501**, 895–910 (1998). doi: 10.1086/305854
8. H. P. Warren, A. Winebarger, Small scale structure in the solar transition region. *Astrophys. J.* **535**, L63 (2000). doi: 10.1086/312690
9. H. Oluseyi, M. Carpio, J. Sheung, Implausibility of hydrostatic funnels constituting the Sun's upper transition region. *Sol. Phys.* **245**, 69–85 (2007). doi: 10.1007/s11207-007-9023-5
10. S. Patsourakos, P. Gouttebroze, A. Vourlidas, The quiet sun network at subarcsecond resolution: VAULT observations and radiative transfer modeling of cool loops. *Astrophys. J.* **664**, 1214–1220 (2007). doi: 10.1086/518645
11. B. De Pontieu *et al.*, The Interface Region Imaging Spectrograph (IRIS). *Sol. Phys.* **289**, 2733–2779 (2014). doi: 10.1007/s11207-014-0485-y
12. J. R. Lemen *et al.*, The Atmospheric Imaging Assembly (AIA) on the Solar Dynamics Observatory (SDO). *Sol. Phys.* **275**, 17–40 (2012). doi: 10.1007/s11207-011-9776-8
13. J. Martínez-Sykora, B. De Pontieu, P. Testa, V. Hansteen, Forward modeling of emission in Solar Dynamics Observatory/ atmospheric imaging assembly passbands from dynamic three-dimensional simulations. *Astrophys. J.* **743**, 23 (2011). doi: 10.1088/0004-637X/743/1/23
14. Materials and Methods are available as supplementary materials on *Science* Online.
15. S. Antiochos, G. Noci, The structure of the static corona and transition region. *Astrophys. J.* **301**, 440 (1986). doi: 10.1086/163912
16. J. Dowdy Jr., D. Rabin, R. Moore, On the magnetic structure of the quiet transition region. *Sol. Phys.* **105**, 35–45 (1986). doi: 10.1007/BF00156374
17. J. A. Klimchuk, S. K. Antiochos, J. T. Mariska, A numerical study of the nonlinear thermal stability of solar loops. *Astrophys. J.* **320**, 409 (1987). doi: 10.1086/165554
18. V. Hansteen, H. Hara, B. De Pontieu, M. Carlsson, On redshifts and blueshifts in the transition region and corona. *Astrophys. J.* **718**, 1070–1078 (2010). doi: 10.1088/0004-637X/718/2/1070
19. N. Guerreiro, V. Hansteen, B. De Pontieu, The cycling of material between the solar corona and chromosphere. *Astrophys. J.* **769**, 47 (2013). doi: 10.1088/0004-637X/769/1/47
20. D. Spadaro, A. F. Lanza, J. T. Karpen, S. K. Antiochos, A transient heating model for the structure and dynamics of the solar transition region. *Astrophys. J.* **642**, 579–583 (2006). doi: 10.1086/500963
21. J. Klimchuk, On solving the coronal heating problem. *Sol. Phys.* **234**, 41–77 (2006). doi: 10.1007/s11207-006-0055-z
22. B. Lites *et al.*, The horizontal magnetic flux of the quiet-sun internetwork as observed with the Hinode spectro-polarimeter. *Astrophys. J.* **672**, 1237–1253 (2008). doi: 10.1086/522922

23. M. J. Martínez González, M. Collados, B. Ruiz Cobo, S. K. Solanki, Low-lying magnetic loops in the solar internetwork. *Astron. Astrophys.* **469**, L39–L42 (2007). doi: 10.1051/0004-6361:20077505

24. J. Sánchez Almeida *et al.*, Search for photospheric footpoints of quiet Sun transition region loops. *Astron. Astrophys.* **475**, 1101–1109 (2007). doi: 10.1051/0004-6361:20078124

25. C. J. Schrijver, A. M. Title, The magnetic connection between the solar photosphere and the corona. *Astrophys. J.* **597**, L165–L168 (2003). doi: 10.1086/379870

26. J. Martínez-Sykora, V. Hansteen, M. Carlsson, Twisted flux tube emergence from the convection zone to the corona. II. Later states. *Astrophys. J.* **702**, 129–140 (2009). doi: 10.1088/0004-637X/702/1/129

SUPPLEMENTARY MATERIALS

www.sciencemag.org/content/346/6207/1255757/suppl/DC1
Materials and Methods
Supplementary Text
Fig. S1
Table S1
Movies S1 to S6
References (*27–31*)

**The unresolved fine structure resolved: IRIS observations of the
solar transition region**